Available online at www.sciencedirect.com
SCIENCE DIRECT
Biochemical and Biophysical Research Communications 343 (2006) 21–26
BBRC
www.elsevier.com/locate/ybbrc

Solution structure and dynamics of Ufm1, a ubiquitin-fold modifier 1

Hiroaki Sasakawa [a,b], Eri Sakata [b], Yoshiki Yamaguchi [b], Masaaki Komatsu [c,d], Kanako Tatsumi [c], Eiki Kominami [d], Keiji Tanaka [c], Koichi Kato [a,b,*]

[a] Institute for Molecular Science, Okazaki National Research Institutes, Higashiyama Myodaiji, Okazaki, Aichi 444-8787, Japan
[b] Graduate School of Pharmaceutical Sciences, Nagoya City University, 3-1 Tanabe-dori, Mizuho-ku, Nagoya 467-8603, Japan
[c] Tokyo Metropolitan Institute of Medical Science, 3-18-22 Honkomagome, Bunkyo-ku, Tokyo 113-8613, Japan
[d] Department of Biochemistry, Juntendo University School of Medicine, 2-1-1 Hongo, Bunkyo-ku, Tokyo 113-8421, Japan

Received 13 February 2006
Available online 28 February 2006

Abstract

The ubiquitin-fold modifier 1 (Ufm1) is one of various ubiquitin-like modifiers and conjugates to target proteins in cells through Uba5 (E1) and Ufc1 (E2). The Ufm1-system is conserved in metazoa and plants, suggesting its potential roles in various multicellular organisms. Herein, we analyzed the solution structure and dynamics of human Ufm1 (hsUfm1) by nuclear magnetic resonance spectroscopy. Although the global fold of hsUfm1 is similar to those of ubiquitin (Ub) and NEDD8, the cluster of acidic residues conserved in Ub and NEDD8 does not exist on the Ufm1 surface. ^{15}N spin relaxation data revealed that the amino acid residues of hsUfm1 exhibiting conformational fluctuations form a cluster at the C-terminal segment and its spatial proximity, which correspond to the versatile ligand-binding sites of Ub and other ubiquitin-like proteins (Ubls). We suggest that Ub and other Ubl-modifiers share a common feature of potential conformational multiplicity, which might be associated with the broad ligand specificities of these proteins.

Keywords: Ufm1; Dynamics; NMR; Ubiquitin; Ubiquitin-like protein

Covalent modification of cellular proteins with ubiquitin (Ub) occurs in eukaryotic cells and regulates a vast array of biological processes including protein degradation, cell-cycle control, stress response, DNA repair, and transcriptional regulation [1]. Eukaryotes express a set of molecules called ubiquitin-like proteins (Ubl) that have structural similarities to Ub. Ubl proteins can be divided into two classes: the type-1 Ubls (e.g., SUMO and NEDD8) are ligated to target molecules in a manner similar, but not identical, to the ubiquitylation pathway, while type-2 Ubls (also called UDPs, ubiquitin-domain proteins, e.g., Rad23, Parkin, and HOIL-1) contain a ubiquitin-like structure embedded in a variety of different classes of large proteins with apparently distinct functions [2–8]. Ub and type-1 Ubls are conjugated covalently to the target substrate(s) by isopeptide linkage between their carboxyl termini and amino groups of lysine residues of acceptor molecules [3,4,9,10].

Recently, a novel type-1 Ubl, which shares 16% sequence identity with Ub, was identified and termed Ufm1 [11]. While Ub and many Ubls possess the conserved C-terminal di-glycine that is adenylated by each specific E1 or E1-like enzyme, respectively, in an ATP-dependent manner, Ufm1(1-83) possesses a single glycine at its C-terminus, which is followed by a Ser-Cys dipeptide in the precursor form of Ufm1. The C-terminally processed Ufm1(1-83) is specifically activated by an E1-like enzyme, Uba5, and then transferred to its cognate E2-like enzyme, Ufc1. The Ufm1-system is conserved in metazoa and plants but not in yeast, suggesting important roles in various multicellular organisms. However, the molecular mechanism of the Ufm1-system on structural basis is still unknown except for the NMR (nuclear magnetic

* Corresponding author. Fax: +81 52 836 3447.
E-mail address: kkato@phar.nagoya-cu.ac.jp (K. Kato).

0006-291X/$ - see front matter © 2006 Elsevier Inc. All rights reserved.
doi:10.1016/j.bbrc.2006.02.107

resonance) structure of protein ZK652.3, the *Caenorhabditis elegans* homologue of hsUfm1 (ceUfm1) [12]. Additionally, although three-dimensional (3D) structure data of Ubl proteins have been reported [6,7,13,14], little is known about conformational dynamics of these proteins, which is generally considered to be an important factor for our understanding of the underlying mechanisms in molecular recognition [15–18]. So far, ^{15}N spin relaxation data have been reported only for Ub and the Ubl domain of human DC-UbP, a type-2 Ubl, but not for type-1 Ubls [19,20]. Here, we report the solution structure and ^{15}N spin relaxation data of the C-terminally processed human Ufm1. This information provides the basis for molecular recognition by this protein.

Materials and methods

Protein expression and purification. The DNA fragment encoding human Ufm1(1-83) was cloned into pGEX6P-1 (Amersham Biosciences, Arlington Heights, IL) to encode the N-terminal GST fusion protein and expressed in *Escherichia coli* strain BL21 CodonPlus(DE3) (Stratagene, La Jolla, CA). Uniformly ^{15}N- and $^{13}C/^{15}N$-labeled proteins were produced and purified as described previously [11] with minor modifications. Briefly, cells were grown in M9 minimal media containing [^{15}N]NH_4Cl and/or [$^{13}C_6$]glucose according to standard protocols. GST-fused protein was purified from cell lysate using a glutathione–Sepharose column (Amersham Biosciences). After cleavage with PreScission Protease (Amersham Biosciences), GST was removed by the application of the digested products onto a second glutathione–Sepharose column. Further purification of the protein was carried out by gel-filtration column. The samples for NMR experiments were prepared at a concentration of 0.2 mM in 90% H_2O/10% D_2O (v/v), 10 mM sodium phosphate buffer, and 100 mM NaCl at pH 6.0.

NMR measurements and spectral analysis. NMR experiments were performed at 303 K using JEOL JNM-ECA920, Bruker Avance 600, and DMX-500 spectrometers equipped with 5-mm triple-resonance probes. Backbone assignments were obtained with HNCA, HN(CO)CA, HNCO, HN(CA)CO, HNCACB, and CBCA(CO)NH experiments [21,22]. Side chain assignments were derived from HCCH-COSY, HCCH-TOCSY, and ^{15}N-edited TOCSY experiments [23]. Hydrogen bond restraints were obtained from ^{1}H-^{15}N-HSQC spectra by hydrogen-deuterium exchange reaction in 99.9% D_2O. NOE restraints were obtained from ^{1}H-^{1}H NOESY, ^{15}N-edited NOESY, and ^{13}C-edited NOESY spectra. The ^{15}N longitudinal spin-relaxation rates (R_1) were measured with relaxation delays of 20, 50, 100, 200, 400, 600, 900, 1200, and 1500 ms. The ^{15}N transverse relaxation rates (R_2) were obtained with ^{15}N 180° CPMG pulses at total relaxation delays of 16, 32, 48, 64, 96, 128, and 240 ms. For R_2 measurements, temperature-compensating ^{15}N 180° pulses were applied during the recycle delay. $^{15}N\{^{1}H\}$ NOEs were obtained by interleaving pulse sequences with and without proton saturation. The time domain data were processed with nmrPipe software package [24]. Semiautomatic assignment of the resonance peaks of each amino acid residue was carried out using the Olivia software (http://fermi.pharm.hokudai.ac.jp/olivia/). Relaxation data were analyzed with Modelfree 4.1 [25] and FASTModelfree [26].

Structure calculations. Backbone dihedral angle restraints for ϕ and φ were created by using TALOS [27]. NOE assignments and structure calculation were performed by CYANA2.0 [28]. Each hydrogen bond was represented by two distance upper limit restraints (N–O and HN–O) to preserve linear bond geometry. A total of 100 random structures were calculated and the 10 lowest target function structures were selected to represent the 3D structure of Ufm1. The calculated structures were validated using the PROCHECK-NMR software [29]. The coordinates have been deposited in the Protein Data Bank (Accession Code 1WXS).

Results and discussion

Solution structure of Ufm1

The final structure of hsUfm1 was calculated with total of 723 distance restraints, 38 hydrogen bonds information, and 100 backbone dihedral angle restraints (Table 1). The resulting root mean square deviation (r.m.s.d.) from the mean structure for backbone atoms was 0.571 Å, which was sufficient to determine the overall structure of hsUfm1. A stereo view of the structure thus obtained is shown in Fig. 1. HsUfm1 assumes a ubiquitin-fold in which Lys3-Thr9 (β1), Val20-Pro24 (β2), Ser47-Thr51 (β3), and Glu73-Pro78 (β5) form β-strands, while Pro29-Glu39 (α1) and Ala63-Lys69 (α2) form α-helices. In a typical Ub fold, β3 and α2 are connected by a short β-strand (β4), which is ambiguous in the Ufm1 structure, probably because two glycine residues (Gly54 and Gly56) in the corresponding segment preclude the formation of a stable β-strand.

The structure of β1–β2 loop (residues 16–23) was not converged due to insufficient NOE constrains. The hydrophobic core of hsUfm1 is formed with Phe6, Ile8, Leu10, Leu21, Val23, Phe29, Val32, Leu33, Phe40, Val45, Ile49, Ile50, Ile57, Val66, Phe67, Leu74, and Ile76. While ceUfm1 has a non-conservative Pro-substitution of Thr at position 62 in hsUfm1 and elongated sequences at both N- and C-terminal regions, its structural feature is similar to that of hsUfm1. The surface electrostatic potential of hsUfm1 is markedly different from those of Ub and NEDD8 (Fig. 2). The most striking feature in hsUfm1 is the non-existence of the cluster of the acidic residues of the α1 surface displayed by Ub and NEDD8. It has recently been reported that the deep grooves between β2-strand and α1-helix of Ubls are subjected to protein–protein interactions [30,31]. It is possible that Ufm1 employs the uncharged surface to bind its putative partner(s).

Table 1
Structural data of human Ufm1

Restraints used in the structure calculation	
Number of distance restraints	723
Number of hydrogen bonds	38
Number of torsion angle restraints	
ϕ	50
ψ	50
Geometric statistics	
R.m.s.d. from the mean structure[a] (Å)	
Backbone atoms (residues 8–15 and 24–82)	0.571
All heavy atoms (residues 8–15 and 24–82)	1.069
Ramachandran analysis (%)	
Most favored regions	74.7
Additional allowed regions	21.5
Generously allowed regions	3.2
Disallowed regions	0.7

[a] Mean coordinates were obtained by averaging coordinates of the 10 calculated structures.

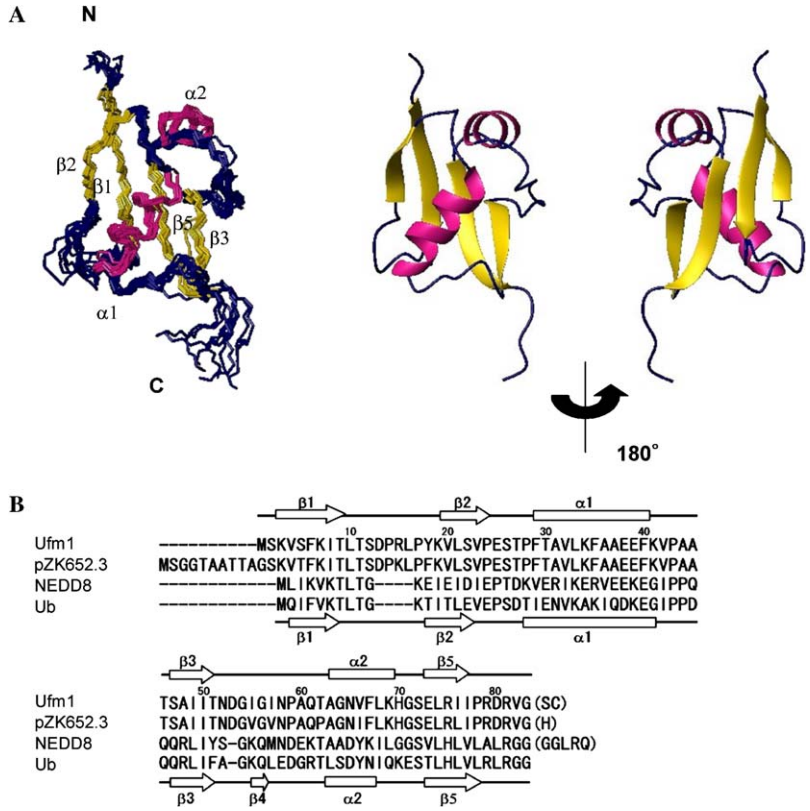

Fig. 1. (A) Backbone atom superposition of the final 10 structures (left) and ribbon representation of the lowest energy structure (right) of hsUfm1. In (A), the structures are superimposed adopting the residues 8–15 and 24–83. The α-helices and β-strands are colored in magenta and yellow, respectively. The graphics were generated by MOLMOL program [45]. (B) Sequence alignment of hsUfm1, protein ZK652.3 (ceUfm1), hsNEDD8, and hsUb. The residue number is labeled according to the sequence of hsUfm1 and the secondary structural elements are displayed for hsUfm1 (top) and hsUb (bottom). The C-terminal residues in parentheses were post-translationally removed.

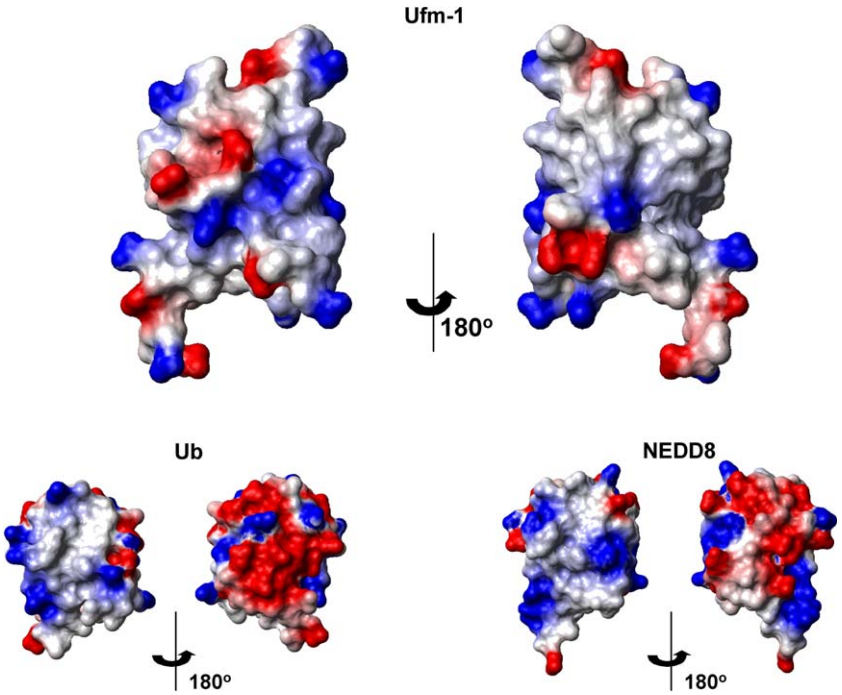

Fig. 2. Comparison of the electrostatic surfaces of hsUfm1, hsUb (PDB code: 1D3Z), and hsNEDD8 (PDB code: 1NDD). The orientation of hsUfm1 is exactly the same as that shown in Fig. 1A. The electrostatic surfaces were calculated and colored by MOLMOL software [45]. The positive and negative charges are shown in blue and red, respectively.

Conformational dynamics of Ufm1

To characterize the solution dynamics of hsUfm1, three ^{15}N spin relaxation parameters (longitudinal relaxation rate R_1, transverse relaxation rate R_2, and $^{15}N\{^1H\}$ NOE) were measured for individual backbone amide groups. From the model-free analysis, the order parameters S^2 and the exchange contribution R_{ex} were computed (Fig. 3). The residues in the N-terminal β1-strand (Lys7 and Ile8), the α1–β3 loop (Val42, Ala44, Ala45, and Thr46), and the C-terminal β5-strand (Arg75 and Ile77) of hsUfm1 displayed higher ($>10\ s^{-1}$) R_{ex} values. In addition, the residues located in the β1–β2 loop (Thr9-Tyr18) exhibited significant broadening of ^1H-^{15}N HSQC peaks, indicating conformational fluctuation in this region. Variable pressure NMR analyses revealed that Ub undergoes conformational fluctuations at the α1–β3 loop and the C-terminal segment at 3 kbar, although such phenomena were not observed at normal pressures [32]. It has been reported that within the structure of the type-2 Ubl of DC-UbP, residues showing higher R_2 values (also high R_2/R_1) form

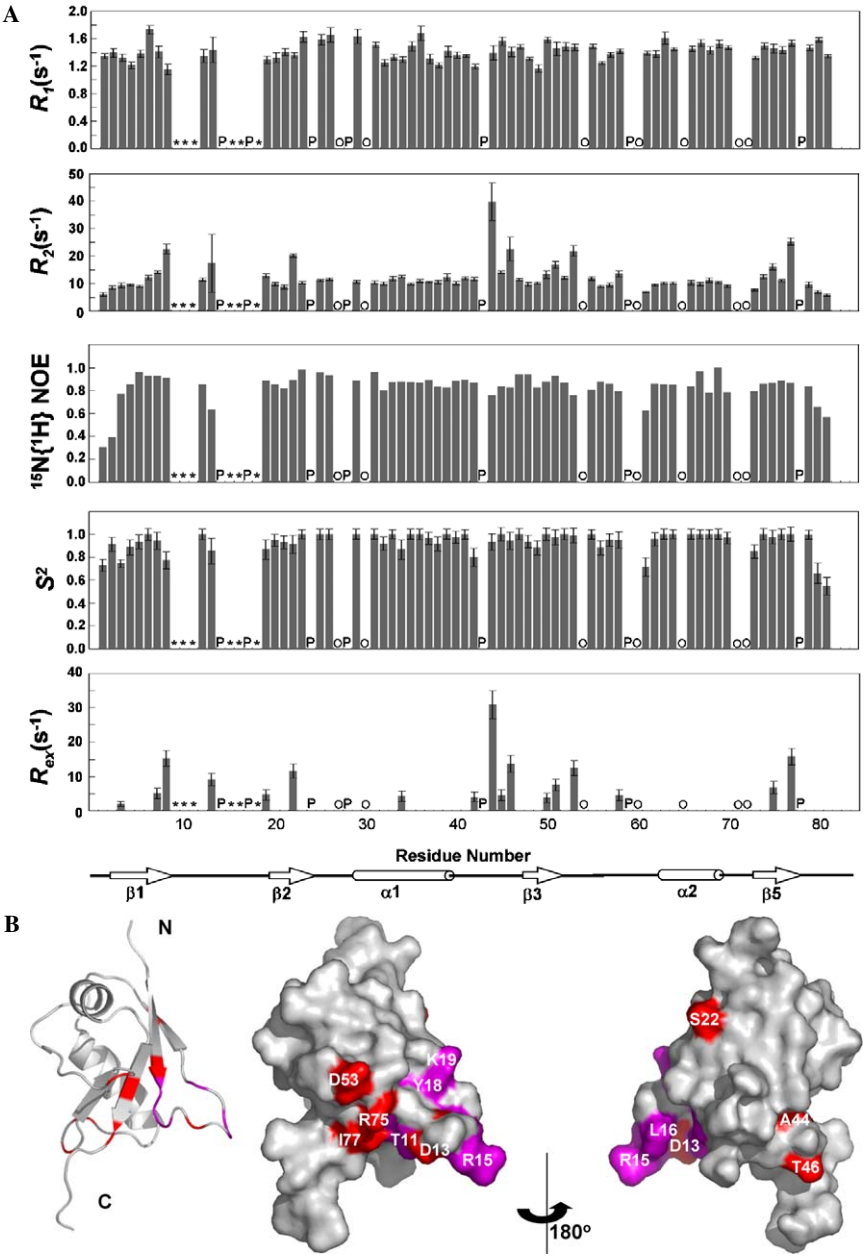

Fig. 3. (A) Summary of ^{15}N spin relaxation data. Asterisk and 'O' indicate residues whose relaxation data could not be obtained due to severe broadening and peak overlapping, respectively, while 'P' represents proline residue. NMR data were measured at a ^1H frequency of 920 MHz. (B) Mapping of residues exhibiting higher R_{ex} values of hsUfm1. Residues exhibiting higher ($>10\ s^{-1}$) R_{ex} values and those indicated with asterisks in (A) are shown in red and magenta, respectively.

a cluster on the surface area that is distinct from the region showing the conformational fluctuation in hsUfm1. These data suggest that Ub and type-1 but not type-2 Ubls share a common feature of (potential) conformational multiplicities, which are more pronounced for hsUfm1.

The amino acid residues exhibiting higher R_{ex} values form a cluster in the C-terminal segment and its spatial proximity of hsUfm1. Accumulating evidence indicates that Ub and Ubls perform versatile protein-protein interactions using the corresponding region, the so-called ''the Ile44 surface'' [33]. The biological functions of Ub and Ubls are mediated by interactions with their acceptor proteins containing the UBA, UIM, CUE, GAT, and/or NZF motifs, which bind the Ile44 surfaces of Ub and some Ubls [6,7,33–41]. The crystallographic data of NEDD8-Appbp1/Uba3, SUMO-Sae1/Sae2, and YUH1-ubiquitin aldehyde complexes indicate that Ub and Ubls also interact with E1 and de-ubiquitinating enzymes as well as their cognate enzymes through the Ile44 surface and C-terminal segments [42–44]. Conformational fluctuations of the ligand-binding sites of Ub and type-1 Ubls are intriguing because they might be associated with broad ligand specificities of these proteins. Further systematic studies on solution structure and dynamics of type-1 and type-2 Ubls could provide structural basis for molecular recognition of these unique classes of proteins.

Acknowledgments

We thank Drs. M. Yokochi and F. Inagaki (Hokkaido University) for generously providing the Olivia program. This work was supported in part by the Protein 3000 project and by Grants-in-Aid from the Ministry of Education, Culture, Sports, Science and Technology of Japan.

References

[1] A. Hershko, A. Ciechanover, The ubiquitin system, Annu. Rev. Biochem. 67 (1998) 425–479.
[2] K. Tanaka, T. Suzuki, T. Chiba, The ligation systems for ubiquitin and ubiquitin-like proteins, Mol. Cells 8 (1998) 503–512.
[3] D.C. Schwartz, M. Hochstrasser, A superfamily of protein tags: ubiquitin, SUMO and related modifiers, Trends Biochem. Sci. 28 (2003) 321–328.
[4] S. Jentsch, G. Pyrowolakis, Ubiquitin and its kin: how close are the family ties? Trends Cell Biol. 10 (2000) 335–342.
[5] H. Hiyama, M. Yokoi, C. Masutani, K. Sugasawa, T. Maekawa, K. Tanaka, J.H. Hoeijmakers, F. Hanaoka, Interaction of hHR23 with S5a. The ubiquitin-like domain of hHR23 mediates interaction with S5a subunit of 26S proteasome, J. Biol. Chem. 274 (1999) 28019–28025.
[6] K.J. Walters, M.F. Kleijnen, A.M. Goh, G. Wagner, P.M. Howley, Structural studies of the interaction between ubiquitin family proteins and proteasome subunit S5a, Biochemistry 41 (2002) 1767–1777.
[7] E. Sakata, Y. Yamaguchi, E. Kurimoto, J. Kikuchi, S. Yokoyama, S. Yamada, H. Kawahara, H. Yokosawa, N. Hattori, Y. Mizuno, K. Tanaka, K. Kato, Parkin binds the Rpn10 subunit of 26S proteasomes through its ubiquitin-like domain, EMBO Rep. 4 (2003) 301–306.
[8] K. Yamanaka, H. Ishikawa, Y. Megumi, F. Tokunaga, M. Kanie, T.A. Rouault, I. Morishima, N. Minato, K. Ishimori, K. Iwai, Identification of the ubiquitin-protein ligase that recognizes oxidized IRP2, Nat. Cell. Biol. 5 (2003) 336–340.
[9] A. Varshavsky, The ubiquitin system, Trends Biochem. Sci. 22 (1997) 383–387.
[10] C.M. Pickart, Mechanisms underlying ubiquitination, Annu. Rev. Biochem. 70 (2001) 503–533.
[11] M. Komatsu, T. Chiba, K. Tatsumi, S. Iemura, I. Tanida, N. Okazaki, T. Ueno, E. Kominami, T. Natsume, K. Tanaka, A novel protein-conjugating system for Ufm1, a ubiquitin-fold modifier, EMBO J. 23 (2004) 1977–1986.
[12] J.R. Cort, Y. Chiang, D. Zheng, G.T. Montelione, M.A. Kennedy, NMR structure of conserved eukaryotic protein ZK652.3 from *C. elegans*: a ubiquitin-like fold, Proteins 48 (2002) 733–736.
[13] F.G. Whitby, G. Xia, C.M. Pickart, C.P. Hill, Crystal structure of the human ubiquitin-like protein NEDD8 and interactions with ubiquitin pathway enzymes, J. Biol. Chem. 273 (1998) 34983–34991.
[14] P. Bayer, A. Arndt, S. Metzger, R. Mahajan, F. Melchior, R. Jaenicke, J. Becker, Structure determination of the small ubiquitin-related modifier SUMO-1, J. Mol. Biol. 280 (1998) 275–286.
[15] J.I. Kim, C.J. Lee, M.S. Jin, C.H. Lee, S.G. Paik, H. Lee, J.O. Lee, Crystal structure of CD14 and its implications for lipopolysaccharide signaling, J. Biol. Chem. 280 (2005) 11347–11351.
[16] D. Djuranovic, B. Hartmann, DNA fine structure and dynamics in crystals and in solution: the impact of BI/BII backbone conformations, Biopolymers 73 (2004) 356–368.
[17] J. Ghuman, P.A. Zunszain, I. Petitpas, A.A. Bhattacharya, M. Otagiri, S. Curry, Structural basis of the drug-binding specificity of human serum albumin, J. Mol. Biol. 353 (2005) 38–52.
[18] I. Bertini, V. Calderone, M. Cosenza, M. Fragai, Y.M. Lee, C. Luchinat, S. Mangani, B. Terni, P. Turano, Conformational variability of matrix metalloproteinases: beyond a single 3D structure, Proc. Natl. Acad. Sci. USA 102 (2005) 5334–5339.
[19] D.M. Schneider, M.J. Dellwo, A.J. Wand, Fast internal main-chain dynamics of human ubiquitin, Biochemistry 31 (1992) 3645–3652.
[20] Y.G. Gao, A.X. Song, Y.H. Shi, Y.G. Chang, S.X. Liu, Y.Z. Yu, X.T. Cao, D.H. Lin, H.Y. Hu, Solution structure of the ubiquitin-like domain of human DC-UbP from dendritic cells, Protein Sci. 14 (2005) 2044–2050.
[21] M. Wittekind, L. Mueller, HNCACB, a high-sensitivity 3D NMR experiment to correlate amide-proton and nitrogen resonances with the alpha- and beta-carbon resonances in proteins, J. Magn. Reson. B101 (1993) 201–205.
[22] L.E. Kay, G.Y. Xu, T. Yamazaki, Enhanced-sensitivity triple-resonance spectroscopy with minimal H_2O saturation, J. Magn. Reson. A109 (1994) 129–133.
[23] G.M. Clore, A. Bax, P.C. Driscoll, P.T. Wingfield, A.M. Gronenborn, Assignment of the side-chain ^{1}H and ^{13}C resonances of interleukin-1β using double- and triple-resonance heteronuclear three-dimensional NMR spectroscopy, Biochemistry 29 (1990) 8172–8184.
[24] F. Delaglio, S. Grzesiek, G.W. Vuister, G. Zhu, J. Pfeifer, A. Bax, NMRPipe: a multidimensional spectral processing system based on UNIX pipes, J. Biomol. NMR 6 (1995) 277–293.
[25] A.M. Mandel, M. Akke, A.G. Palmer III, Backbone dynamics of *Escherichia coli* ribonuclease HI: correlations with structure and function in an active enzyme, J. Mol. Biol. 246 (1995) 144–163.
[26] R. Cole, J.P. Loria, FAST-Modelfree: a program for rapid automated analysis of solution NMR spin-relaxation data, J. Biomol. NMR 26 (2003) 203–213.
[27] G. Cornilescu, F. Delaglio, A. Bax, Protein backbone angle restraints from searching a database for chemical shift and sequence homology, J. Biomol. NMR 13 (1999) 289–302.

[28] T. Herrmann, P. Güntert, K. Wüthrich, Protein NMR structure determination with automated NOE-identification in the NOESY spectra using the new software ATNOS, J. Biomol. NMR 24 (2002) 171–189.
[29] R.A. Laskowski, J.A. Rullmann, M.W. MacArthur, R. Kaptein, J.M. Thornton, AQUA and PROCHECK-NMR: programs for checking the quality of protein structures solved by NMR, J. Biomol. NMR 8 (1996) 477–486.
[30] J. Song, Z. Zhang, W. Hu, Y. Chen, Small ubiquitin-like modifier (SUMO) recognition of a SUMO binding motif: a reversal of the bound orientation, J. Biol. Chem. 280 (2005) 40122–40129.
[31] C. Kiel, S. Wohlgemuth, F. Rousseau, J. Schymkowitz, J. Ferkinghoff-Borg, F. Wittinghofer, L. Serrano, Recognizing and defining true Ras binding domains II: in silico prediction based on homology modelling and energy calculations, J. Mol. Biol. 348 (2005) 759–775.
[32] R. Kitahara, S. Yokoyama, K. Akasaka, NMR snapshots of a fluctuating protein structure: ubiquitin at 30 bar–3 kbar, J. Mol. Biol. 347 (2005) 277–285.
[33] M. Kawasaki, T. Shiba, Y. Shiba, Y. Yamaguchi, N. Matsugaki, N. Igarashi, M. Suzuki, R. Kato, K. Kato, K. Nakayama, S. Wakatsuki, Molecular mechanism of ubiquitin recognition by GGA3 GAT domain, Genes Cells 10 (2005) 639–654.
[34] K. Fujiwara, T. Tenno, K. Sugasawa, J.G. Jee, I. Ohki, C. Kojima, H. Tochio, H. Hiroaki, F. Hanaoka, M. Shirakawa, Structure of the ubiquitin-interacting motif of S5a bound to the ubiquitin-like domain of HR23B, J. Biol. Chem. 279 (2004) 4760–4767.
[35] T.D. Mueller, J. Feigon, Structural determinants for the binding of ubiquitin-like domains to the proteasome, EMBO J. 22 (2003) 4634–4645.
[36] G. Prag, S. Misra, E.A. Jones, R. Ghirlando, B.A. Davies, B.F. Horazdovsky, J.H. Hurley, Mechanism of ubiquitin recognition by the CUE domain of Vps9p, Cell 113 (2003) 609–620.
[37] R.S. Kang, C.M. Daniels, S.A. Francis, S.C. Shih, W.J. Salerno, L. Hicke, I. Radhakrishnan, Solution structure of a CUE-ubiquitin complex reveals a conserved mode of ubiquitin binding, Cell 113 (2003) 621–630.
[38] S.L. Alam, J. Sun, M. Payne, B.D. Welch, B.K. Blake, D.R. Davis, H.H. Meyer, S.D. Emr, W.I. Sundquist, Ubiquitin interactions of NZF zinc fingers, EMBO J. 23 (2004) 1411–1421.
[39] Y. Kang, R.A. Vossler, L.A. Diaz-Martinez, N.S. Winter, D.J. Clarke, K.J. Walters, UBL/UBA ubiquitin receptor proteins bind a common tetraubiquitin chain, J. Mol. Biol. 356 (2005) 1027–1035.
[40] Q. Wang, P. Young, K.J. Walters, Structure of S5a bound to monoubiquitin provides a model for polyubiquitin recognition, J. Mol. Biol. 348 (2005) 727–739.
[41] R. Varadan, M. Assfalg, S. Raasi, C. Pickart, D. Fushman, Structural determinants for selective recognition of a Lys48-linked polyubiquitin chain by a UBA domain, Mol. Cell 18 (2005) 687–698.
[42] L.M. Lois, C.D. Lima, Structures of the SUMO E1 provide mechanistic insights into SUMO activation and E2 recruitment to E1, EMBO J. 24 (2005) 439–451.
[43] H. Walden, M.S. Podgorski, D.T. Huang, D.W. Miller, R.J. Howard, D.L. Minor Jr., J.M. Holton, B.A. Schulman, The structure of the APPBP1-UBA3-NEDD8-ATP complex reveals the basis for selective ubiquitin-like protein activation by an E1, Mol. Cell 12 (2003) 1427–1437.
[44] S.C. Johnston, S.M. Riddle, R.E. Cohen, C.P. Hill, Structural basis for the specificity of ubiquitin C-terminal hydrolases, EMBO J. 18 (1999) 3877–3887.
[45] R. Koradi, M. Billeter, K. Wüthrich, MOLMOL: a program for display and analysis of macromolecular structures, J. Mol. Graph. 14 (1996) 51–55.